Journal of Superconductivity: Incorporating Novel Magnetism, Vol. 17, No. 2, April 2004 (© 2004)

Jahn–Teller and the Dynamics of Polaron Formation

S. A. Trugman,[1] Li-Chung Ku,[1,2] and J. Bonča[3]

Received 10 August 2003

We discuss a powerful algorithm for calculating static and dynamic properties of electron–phonon coupled systems with dynamic quantum phonons. The difference between Jahn–Teller polarons present in certain transition metal oxides and simpler Holstein polarons is explored. We calculate the dynamics of polaron formation from a bare injected electron, which has been measured in several recent experiments.

KEY WORDS: polaron formation dynamics; Jahn–Teller polarons; Holstein polarons; thermopower.

1. INTRODUCTION

The problem of even a single itinerant electron coupled to a lattice of quantum dynamical phonons is a many-body problem, in that many phonons are excited at various positions, with nontrivial correlations [1]. Like other many-body problems, polaron problems have been solved numerically by exact diagonalization on a finite lattice [2]. In these approaches, the accuracy increases as

$$\text{error} \sim 1/\log(\text{effort}), \tag{1}$$

where effort signifies computer cycles or memory. Large increases in execution time or computer power yield only modest improvement. Recently, methods have become available that converge far more rapidly [3,4], with

$$\text{error} \sim 1/(\text{effort})^{\theta}. \tag{2}$$

The exponent is rather large, $\theta \approx 3$. These newer algorithms are far more accurate, typically by 14 orders of magnitude. The increased power makes it possible to calculate in higher dimensions, $D = 1, 2, 3, 4$, and for more complicated Hamiltonians, such as the Jahn–Teller Hamiltonian relevant to transition metal oxides, in which there is an extra electron orbital and extra phonon degree of freedom coupled in a symmetrical way. The method is variational on an infinite lattice, works at any momentum $\vec{k}$, and provides wavefunctions to calculate arbitrary expectation values. (The three-point functions are surprising and require a new picture of a polaron's phonon cloud [4].) Properties for nonlinear phonons, long-range Fröhlich interactions, bipolarons, the isotope effect, excited states, and dynamics far from equilibrium can be calculated.

The Hamiltonian for the single electron Holstein polaron is

$$\begin{aligned} H &= H_{\text{el}} + H_{\text{el–ph}} + H_{\text{ph}} \\ &= -t \sum_{\langle i,j \rangle} \left(c_i^{\dagger} c_j + hc \cdot \right) \\ &\quad - \lambda \sum_j c_j^{\dagger} c_j \left(a_j + a_j^{\dagger} \right) + \omega_0 \sum_j a_j^{\dagger} a_j, \end{aligned} \tag{3}$$

where $c_j^{\dagger}$ creates an electron and $a_j^{\dagger}$ creates a phonon on site j. The parameters of the model are the nearest-neighbor hopping integral t, the el–ph coupling strength λ, and the phonon frequency ω_0. The electron couples to a dispersionless optical phonon mode on every site. We also consider the more complicated Jahn–Teller (JT) polaron, relevant to transition metal oxides including cuprates and CMR manganites,

[1]Theoretical Division, Los Alamos National Laboratory, Los Alamos, New Mexico 87545.
[2]Department of Physics, University of California, Los Angeles, California 90024.
[3]FMF, University of Ljubljana and J. Stefan Institute, 1000, Ljubljana, Slovenia.

0896-1107/04/0400-0193/0 © 2004 Plenum Publishing Corporation

$$
\begin{aligned}
H_{\mathrm{JT}} &= H_{\mathrm{el}} + H_{\mathrm{el-ph}} + H_{\mathrm{ph}} \\
&= -\sum_{\langle i,j\rangle,\mathrm{X},\mathrm{Y}} t^{\mathrm{X},\mathrm{Y}} (c^{\dagger}_{i,\mathrm{X}} c_{j,\mathrm{Y}} + hc\cdot) \\
&\quad - \lambda \sum_i [(c^{\dagger}_{i,a} c_{i,a} - c^{\dagger}_{i,b} c_{i,b})(a_{i,3} + a^{\dagger}_{i,3}) \\
&\quad + (c^{\dagger}_{i,a} c_{i,b} + c^{\dagger}_{i,b} c_{i,a})(a_{i,2} + a^{\dagger}_{i,2})] \\
&\quad + \omega_0 \sum_i (a^{\dagger}_{i,2} a_{i,2} + a^{\dagger}_{i,3} a_{i,3}), \qquad (4)
\end{aligned}
$$

where $c^{\dagger}_{j,\mathrm{X}}$ creates an electron in orbital X and $a^{\dagger}_{j,\mathrm{m}}$ creates a phonon (of type m) on site j. Indices X and Y are summed over the two e_g orbitals. The electron is coupled to two dispersionless optical phonons on each site, modes Q_2 and Q_3, with creation operators $a^{\dagger}_2$ and $a^{\dagger}_2$.

In section 2, we consider how Jahn–Teller polarons differ from Holstein polarons, and in section 3, the dynamics of polaron formation. Other problems, for example those containing important spin degrees of freedom, can be solved by similar methods.

2. JAHN–TELLER POLARONS

Recent studies have clarified how the extra electron and phonon modes give the quantum dynamical Jahn–Teller polaron different properties from the simpler Holstein polaron [5–8]. As the electron–phonon coupling λ increases, the JT polaron is at first heavier, but ultimately lighter than the Holstein polaron at strong coupling. The finite frequency conductivity of the JT polaron is richer and less clustered around harmonics of ω_0 than the Holstein polaron, because of nonlinear phonon effects. Some other properties are broadly similar.

There may be qualitative differences between Jahn–Teller and Holstein polarons more striking than those discussed in the above references. The "Mexican hat" potential in the (Q_2, Q_3) phonon plane has a sharp point at the crown [9], and is thus highly nonlinear. When quantized, the singular potential leads to nonlinear phonon processes, in which for example a high frequency phonon is converted to two lower frequency phonons. Such conversions dominate certain physical processes such as the ultrafast dynamics of superconducting condensate formation, in which phonons of energy greater than 2Δ continue to break Cooper pairs until they decay into lower frequency phonons (the "phonon bottleneck") [10,11]. The condensate should form more quickly in the presence of non-pairbreaking JT impurities.

In addition to the center of mass momentum, the low energy excitations of a Jahn–Teller polaron are angular modes around the minimum of the Mexican hat. These modes are much lower in frequency than the bare phonon ω_0 for strong electron–phonon coupling, and have no analog in Holstein or Fröhlich polarons. It was shown in 1958 by Longuet–Higgins *et al.* that the allowed angular quantum numbers J are not the integers $\ldots, -2, -1, 0, 1, 2, \ldots$, but rather the half integers $\ldots, -\frac{3}{2}, -\frac{1}{2}, \frac{1}{2}, \frac{3}{2}, \ldots$ [12]. The half integers are due to what would now be called a Berry phase, which effectively puts half a flux quantum through the center of the Mexican hat. A simple way to see this is to follow the ground state of $H = -\cos(\phi)\sigma_x - \sin(\phi)\sigma_z$ as ϕ varies from 0 to 2π, where σ are the 2×2 σ-matrices implicit in the λ term of Eq. 4. The ground state acquires a minus sign, for the same reason that electrons do under 2π rotation.

The ground state is thus two-fold degenerate, in addition to any spin degeneracy. This $J = \pm\frac{1}{2}$ "pseudospin" degeneracy persists for strong electron–phonon coupling, when nonlinear terms cause the Mexican hat to develop three weak minima [9]. (Compare a three-site tight-binding ring, which has a two-fold degenerate ground state when a half flux quantum threads the ring.) Dilute localized Jahn–Teller impurities should thus have residual entropy at zero or low temperature, analogous to free spins. They may order at low temperatures via strain-induced interactions among the pseudospins. A magnetic field lifts the degeneracy between true spin up and down, causing a Curie spin susceptibility χ that diverges at low temperatures as $1/T$. Similarly, shear strain lifts the degeneracy between the pseudospin states in dilute Jahn–Teller systems, and should lead to a $1/T$ divergence in the shear modulus C_{12}. Because it couples to local lattice strain, the pseudospin degree of freedom may become "incoherent" faster than ordinary spin, and thus be less suitable for quantum computing.

A mobile Jahn–Teller polaron can change its angular quantum number J when scattering from an impurity, because local strain fields couple to J. There is little energy cost in changing J (much less than the optical phonon frequency ω_0), so collisions with impurities are often weakly inelastic. The J and $-J$ states are energetically degenerate. The many scattering channels should reduce the effects of weak localization, which require "coherent" interference. The scattering of Jahn–Teller polarons stands in contrast to free electrons that scatter elastically from impurities, and Holstein polarons that more often scatter elastically because they lack low energy internal modes.

As a Jahn–Teller polaron moves, it carries with it internal vibrational energy (the angular J modes at low temperature). In these systems, heat or vibrational energy can thus be moved from place to place by an electric field that couples to the polaron charge. This should be a much stronger effect than ordinary "phonon drag," because the vibrational excitations are actually bound to the charge carriers rather than merely scattering from them. This should lead to a large thermopower anomaly, with possible applications in thermoelectric refrigeration. Related effects occur in Holstein polaron systems, where bound states of a polaron and thermally excited phonons occur at sufficiently strong coupling λ [3,13]. These are, however, higher energy states in Holstein systems, closer to an optical phonon energy. It would be interesting to confirm or refute these suggestions experimentally. Scattering of phonons by Jahn–Teller polarons has been observed [14].

3. DYNAMICS OF POLARON FORMATION

The question of how a bare electron becomes a polaron has been the subject of recent experiments [15–19]. The time to form a polaron is found to be less than a picosecond in strongly coupled systems, on the order of a phonon period. We consider this issue theoretically. One approach is to construct a variational many-body Hilbert space including multiple phonon excitations, and to numerically solve the many-body Schrödinger Equation

$$i\frac{d\psi}{dt} = H\psi \tag{5}$$

in this space. The main approximation is the size of the variational space, which can be increased systematically until convergence is achieved. This method includes the full quantum dynamics. Alternative treatments, such as the semiclassical approximation, can be inaccurate. We have solved for the dynamics where H is the 1D Holstein Hamiltonian Eq. 3 and the phonons are initially at zero temperature, shown in Fig. 1. A bare electron wavepacket moving right is injected at time zero. In panel (c) after an elapsed time of one phonon period, the electron density consists of two peaks. The peak on the right (light arrow) is essentially a bare electron. The peak on the left heavy arrow is a polaron wavepacket moving more slowly. As time goes on, the bare electron peak decays and the polaron peak grows. Some phonons are left behind mainly near the injection point (heavy dashed line). These phonons are of known phase (dot-dashed line). Some phonon excitations travel with the polaron (heavy dot-dashed line).

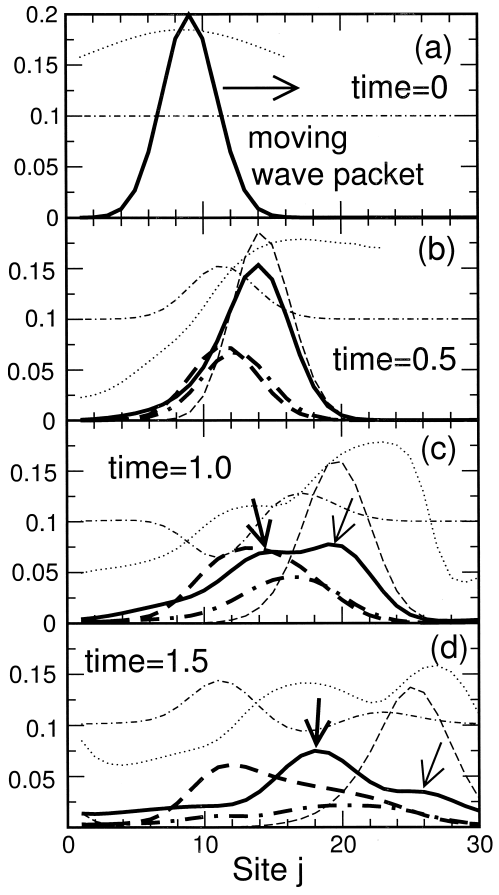

Fig. 1. (a)–(d) Snapshots of the polaron-formation process, for $t = \omega_0 = 1$, and $\lambda = 0.4$. The calculation is performed on a 30-site periodic lattice. Time is measured in phonon periods. Heavy solid: electron density $\langle c_j^\dagger c_j \rangle$; Heavy dashed: phonon density $\langle a_j^\dagger a_j \rangle$; Dot-dashed: lattice displacement $\langle a_j + a_j^\dagger \rangle$; Dotted: velocity in units of lattice constant per phonon period; Heavy dot-dashed: el–ph correlation function $\langle c_j^\dagger c_j a_j^\dagger a_j \rangle$ Dashed: free-electron wave packet for reference. For clarity, the origins of the dot-dashed and dotted curves are offset by 0.1 and their values are rescaled by a factor of 0.2 and $0.05/(2\pi)$ respectively.

There are regimes where the polaron formation time is a calculable constant of order unity times a phonon period T_0, as shown in Fig. 1, but there are other regimes where the phonon period is not the relevant timescale. The limit hopping $t \to 0$ is instructive. After a time $T_0/4$ the expectation of the phonon coordinate $\langle x_j \rangle$ on the electron site has the same value as a static polaron. It is tempting (but we would argue incorrect) to identify this as the polaron formation time. At later times, $\langle x_j \rangle$ overshoots by a factor of two, and after time T_0, $\langle x_j \rangle$ and all other correlations are what they were at time zero when the bare

electron was injected. The system oscillates forever. In general an electron emits phonons enroute to becoming a polaron, and we propose that the polaron formation time be defined as the time required for the polaron to physically separate from the radiated optical phonons. The polaron formation time for hopping $t \to 0$ is then infinite, because the polaron is forever stuck on the same site as the radiated phonons. Another instructive example is an electron injected at several times the phonon energy ω_0 above the bottom of the band. The electron radiates successive phonons to reduce its kinetic energy to near the bottom of the band, and then forms a polaron. For weak electron–phonon coupling λ, the first phonon is radiated at a rate proportional to λ^2 by Fermi's golden rule, which for small λ is a time arbitrarily longer than the phonon period T_0.

We now consider polaron formation in more detail. After injecting a bare electron at time zero, the wavefunction at later times is

$$|\psi(t)\rangle = \sum_{j=1}^{\infty} e^{-iE_j t} |\Psi_j\rangle \langle \Psi_j | c_k^\dagger | 0 \rangle, \tag{6}$$

where $|\Psi_j\rangle$ are a complete set of total momentum k eigenstates of the system of one electron coupled to phonons. There are several distinct types of states contributing to the infinite sum:

(a) The state $|k\rangle$ of a momentum k polaron, corresponding to the quasiparticle pole.

(b1) The states $|k - q_1; q_1\rangle$ corresponding to a polaron of momentum $k - q_1$ and an unbound phonon of momentum q_1, for any q_1.

(b2 . . .) The states $|k - q_1 - q_2; q_1, q_2\rangle$ corresponding to a polaron of momentum $k - q_1 - q_2$ and unbound phonons of momentum q_1 and q_2 for any q_1 and q_2, and similarly for 3 or more unbound phonons.

If the electron–phonon coupling is sufficiently strong, there are additional states in the sum:

(a*) A polaron excited state consisting of a polaron and an additional bound phonon of total momentum k, designated $|k^*\rangle$. This is a second type of (excited) quasiparticle pole that is also split off from the continuum.

(b1* . . .) The states $|k - q_1^*; q_1\rangle$ corresponding to an excited state polaron of momentum $k - q_1$ and an unbound phonon of momentum q_1 for any q_1. Similarly for two unbound phonons, etc. For stronger electron-phonon coupling, additional polaron excited states corresponding to two or more bound phonons, possibly accompanied by one or more unbound phonons enter the sum as well. The branching ratios into the various channels is calculated in Ref. [8]. Polaron excited states are discussed in references [3,13].

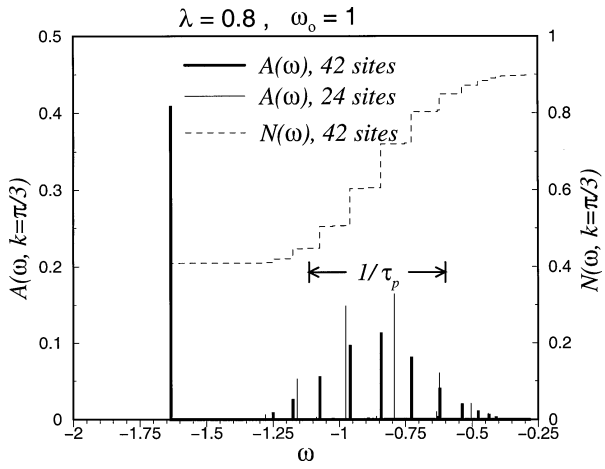

Fig. 2. Spectral function of a Holstein polaron. The quasiparticle pole does not change when the size increases from 24 to 42. The heights of the peaks stand for the intensity of the δ functions. The integrated density of states, $N(\omega, k) = \int_{-\infty}^{\omega} A(\omega', k) d\omega'$. Using the Lanczos algorithm, one obtains numerically exact Ψ_n and ω_n, where n is large enough to contain most of the spectral weight.

From Eq. 6, the amplitude to remain in the initial state after time t, $\langle \psi(t) | c_k^\dagger | 0 \rangle$, is given by the Fourier transform of the spectral function

$$A(k, \omega) = \sum_{j=1}^{\infty} \left| \langle \Psi_j | c_k^\dagger | 0 \rangle \right|^2 \delta(\omega - \omega_j). \tag{7}$$

The numerically determined spectral function at fairly weak coupling is shown in Fig. 2. The sum rule $N(\omega)$ shows that only about 10% of the total spectral weight is at energies beyond the range plotted. There is a quasiparticle pole corresponding to (a) above, and a group of states that is approaching an approximately Lorenzian continuum as the number of sites increases, corresponding to (b1) above. The coupling $\lambda/\omega_0 = 0.8$ is too weak to form bound quasiparticle excited states $|k^*\rangle$. If the spectral function were a pure Lorenzian, a measurement would yield an exponential decay of the initial state $\exp(-t/\tau)$, with the polaron formation time τ the inverse width of the Lorenzian. Since the spectral function has a quasiparticle pole as well, an experiment would measure the probability to remain in the initial state

$$P(t) = a_1^2 + a_2^2 e^{-2bt} + 2a_1 a_2 e^{-bt} \cos[(\omega_1 - \omega_2)t]. \tag{8}$$

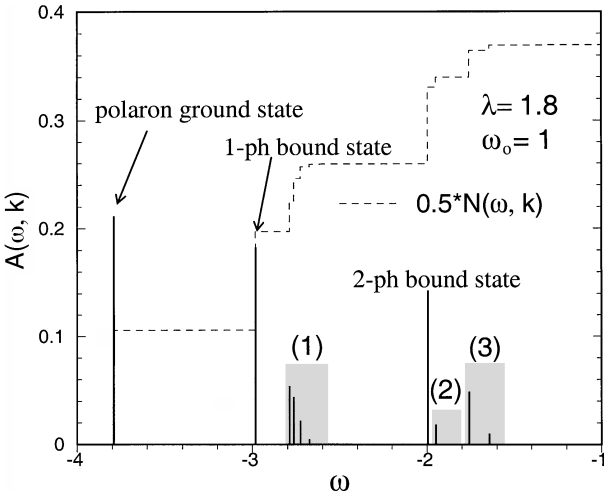

Fig. 3. Spectral function (solid) and the integrated density of states (dashed) in the strong-coupling regime. Shaded regions are unbound phonon excitations: (1) continuum of one unbound phonon plus polaron ground state; (2) continuum of one-phonon bound state plus one unbound phonon; (3) continuum of two unbound phonons plus polaron ground state. The calculation is performed on an infinite lattice but the maximum separation between the electron and phonons is 19 sites. (Number of basis states is 1.8×10^6.) Momentum $k = 0$.

This form already shows some complications, with an additive constant, a pure exponential decay, and an exponential decay half as fast multiplied by a cosine oscillating at the energy difference between the quasiparticle pole and the center of the Lorenzian. Decaying oscillations in polaron formation (actually the formally equivalent problem of an exciton coupled to phonons) have been observed by Sugita *et al.* [17].

A numerically calculated spectral function at stronger coupling is shown in Fig. 3. A polaron and two excited state polaron poles, along with three continua are shown. There is additional structure at higher energy (not shown). The probability $P(t)$ for this spectrum is considerably more complicated, and includes oscillating terms that do not decay to zero (at zero temperature) from the ground and excited polaron poles beating against each other. Further details and results in higher dimensions are given in Ref. [8].

The question "how long does it take a polaron to form?" may not have a simple answer, given the potentially complicated form of $P(t)$. This function can be calculated numerically, and at zero temperature depends on the parameters of the Hamiltonian, the spatial dimension, the initial bare electron momentum k, the final polaron momentum of interest (the initial k or a different momentum?), and the possible existence of bound polaron excited states. A further complication is that decay out of the initial state need not be synonymous with decay into a polaron final state, as seen from the weak coupling λ regime discussed above (Eq. 6). Generalizations of the spectral function can give the required information in these cases.

ACKNOWLEDGMENTS

The authors would like to acknowledge valuable discussions with A. Alexandrov, A. Bishop, D. Khomskii, K. Müller, and A. Taylor.

REFERENCES

1. A. S. Alexandrov and Nevill Mott, *Polarons and Bipolarons* (World Scientific, London, 1995).
2. G. Wellein and H. Fehske, *Phys. Rev. B* **56,** 4513 (1997).
3. J. Bonča, S. A. Trugman, and I. Batistić, *Phys. Rev. B* **60,** 1633 (1999).
4. L.-C. Ku, S. A. Trugman, and J. Bonča, *Phys. Rev. B* **65,** 174306 (2002).
5. S. El Shawish, J. Bonča, L.-C. Ku, and S. A. Trugman, *Phys. Rev. B* **67,** 14301 (2003).
6. Y. Takada, *Phys. Rev. B* **61,** 8631 (2000).
7. P. E. Kornilovich, *Phys. Rev. Lett.* **84,** 1554 (2000).
8. Li-Chung Ku, Ph.D. Thesis, UCLA, 2003.
9. I. B. Bersuker and V. Z. Polinger, *Vibronic Interactions in Molecules and Crystals* (Springer, Berlin, 1989).
10. J. Demsar, B. Podobnik, V. V. Kabanov, T. Wolf, and D. Mihailovic, *Phys. Rev. Lett.* **82,** 4918 (1999).
11. R. D. Averitt, G. Rodriguez, A. I. Lobad, J. L. Siders, S. A. Trugman, and A. J. Taylor, *Phys. Rev. B* **63,** 140502(R) (2001).
12. H. C. Longuet-Higgins, U. Öpik, M. H. L. Pryce, and R. A. Sack, *Proc. R. Soc. A* **224,** 1 (1958).
13. S. Ciuchi, F. de Pasquale, S. Fratini, and D. Feinberg, *Phys. Rev. B* **56,** 4494 (1997).
14. M. Ikebe, H. Fujishiro, and M. Numano, *Physica B* **316–317,** 265 (2002).
15. N.-H. Ge, C. M. Wong, R. L. Lingle Jr., J. D. McNeill, K. J. Gaffney, and C. B. Harris, *Science* **279,** 202 (1998); N.-H. Ge, C. M. Wong, and C. B. Harris, *Acc. Chem. Res.* **33,** 111 (2000).
16. A. D. Miller, I. Bezel, K. J. Gaffney, S. Garrett-Roe, S. H. Liu, P. Szymanski, and C. B. Harris, *Science* **297,** 1163 (2002).
17. A. Sugita, T. Saito, H. Kano, M. Yamashita, and T. Kobayashi, *Phys. Rev. Lett.* **86,** 2185 (2001).
18. R. D. Averitt and A. J. Taylor, *J. Phys. Condens. Matter* **14,** R1357 (2002).
19. R. D. Averitt, V. K. Thorsmolle, Q. X. Jia, and A. J. Taylor, OSA Trends in Optics and Photonics Vol. 79, Nonlinear Optics, OSA Technical Digest (Optical Society of America, Washington DC, 2002) p. 23–25.